Single α-Domain Constructs of the Na^+/Ca^{2+} Exchanger, NCLX, Oligomerize To Form a Functional Exchanger†

Raz Palty,‡ Michal Hershfinkel,§ Oren Yagev, Drorit Saar,‡ Ronit Barkalifa,§ Daniel Khananshvili,|| Asher Peretz,|| Yoram Grossman,‡ and Israel Sekler*,‡

Departments of Physiology and Morphology, Zlotowski Center for Neuroscience, Faculty of Health Sciences, Ben-Gurion University of the Negev, Beer-Sheva 84105, Israel, and Department of Physiology and Pharmacology, Sackler School of Medicine, Tel-Aviv University, Ramat-Aviv 69978, Israel

Received March 31, 2006; Revised Manuscript Received August 4, 2006

ABSTRACT: Spliced isoforms of the Na^+/Ca^{2+} exchanger, NCLX, truncated at the α-repeat region have been identified. The activity and functional organization of such proteins are, however, poorly understood. In the present work, we have studied Na^+/Ca^{2+} exchange mediated by single α-repeat constructs (α1 and α2) of NCLX. Sodium-dependent calcium transport was fluorescently detected in both the reversal and forward modes; calcium-dependent outward currents were also recorded using a whole cell patch configuration in HEK293 cells heterologously expressing either the α1 or α2 single-domain proteins. In contrast, calcium transport and reversal currents were not detected when cells were transfected with a vector or with an α2 mutant (α2-S273T). Thus, our data indicate that the single α-domain constructs mediate electrogenic Na^+/Ca^{2+} exchange. The α1 domain, but not the α2, exhibited partial sensitivity to the NCX inhibitor, KB-R7943, while Li^+-dependent Ca^{2+} efflux was detected in cells expressing either the α1 or α2 construct. The functional organization of the single α-domain constructs was assessed using a dominant-negative approach. Coexpression of the α1 or α2 constructs with the nonfunctional α2-S273T mutant had a synergistic inhibitory effect on Na^+/Ca^{2+} transport. Dose-dependence analysis of the inhibition of α2 construct activity by the α2-S273T mutant indicated that the functional unit is either a dimer or a trimer. Immunoprecipitation analysis indicated that the α2 construct indeed interacts with the α2-S273T mutant. Taken together, our data indicate that although single α1 or α2 domain constructs are independently capable of Na^+/Ca^{2+} exchange, oligomerization is required for their activity. Such organization may give rise to transport activity with distinct kinetic parameters and physiological roles.

Sodium/calcium exchangers play a fundamental role in controlling cellular Ca^{2+} homeostasis by utilizing the transmembrane sodium gradient to exchange three to four Na^+ ions for one Ca^{2+} ion (*1*). Members of the mammalian Na^+/Ca^{2+} exchanger superfamily (NCX1−3, NCKX1−4, and NCLX)[1] share similar organization of two transmembrane domains, designated α1 and α2, separated by an intracellular loop. Recently, a new member of the Na^+/Ca^{2+} exchanger superfamily, encoded by the *FLJ22233* gene, was identified. A study by Cai et al. (*2*) reported that the full-length *FLJ22233* protein, heterologously expressed in HEK293 cells, is retained in the endoplasmic reticulum. A mouse spliced isoform was shown by the same group to mediate active K^+-dependent Na^+/Ca^{2+} exchange. We subsequently showed, however, that the full-length protein encoded by the human *FLJ22233* gene is mediating Na^+/Ca^{2+} exchange that is independent of K^+ ions (*3*). We further demonstrated that *FLJ22233* is distinct from both NCX and NCKX in its ability to catalyze both Na^+/Ca^{2+} and Li^+/Ca^{2+} exchange at a similar rate and have therefore termed it NCLX (Na^+/Ca^{2+}, Li^+ exchanger).

The NCLX shares a relatively low degree (∼20%) of sequence homology with other members of the Na^+/Ca^{2+} superfamily. For example, NCLX lacks the typical long cytoplasmic domain that is found on NCX and has distinct putative arrangement of the transmembrane domains (*2*), but it retains the α1 and α2 regions embedded within the transmembrane domains (*4*). Another distinct phenomenon of NCLX is the abundant and ubiquitous expression of spliced isoforms truncated at their α-domain regions. The spliced isoform of the NCLX mouse homologue gene that has previously been described as a K^+-dependent, Li^+-inert, Na^+/Ca^{2+} exchanger has a disruption of the α2 domain (*2*). We have also identified a short isoform of the human NCLX gene (s-NCLX) with a disrupted α1 domain that is mediating both Na^+/Ca^{2+} and Li^+/Ca^{2+} exchange, similar to the full-length NCLX (*3*). The spliced NCLX isoforms lacking an α domain are even more interesting considering that for NCKX and NCX most of the splicing sites are located at the putative cytoplasmic domains and appear to result in

† This work was supported in part by Binational Science Foundation Grant 2001101 (to M.H.), ISF Grant 456/02.1 (to I.S.), and Israel Science Foundation Equipment Grant 456/02.2 (to I.S.), and R.P. was supported by ISF "Adams" and BGU "Kreitman" fellowships.

* To whom correspondence should be addressed. Tel: 972-8-6477328. Fax: 972-8-6477628. E-mail: sekler@bgu.ac.il.

‡ Department of Physiology, Ben-Gurion University of the Negev.

§ Department of Morphology, Ben-Gurion University of the Negev.

|| Department of Physiology and Pharmacology, Tel-Aviv University.

[1] Abbreviations: NCX, Na^+/Ca^{2+} exchanger; NMG, *N*-methyl-D-glucamine; EDTA, ethylenediaminetetraacetic acid.

10.1021/bi060633b CCC: $33.50
Published on Web 09/12/2006

tissue-specific regulation of NCX activity by calcium or voltage (*5*). Spliced isoforms containing single or disrupted α-repeats of NCX and NCKX, on the other hand, are much less common than those of NCLX. While functional studies exploring the molecular determinants necessary for ion transport in members of both NCX and NCKX (*6*−*8*) have suggested that both α-repeat domains are necessary for ion exchange (*9*, *10*), other studies have suggested that exchange, albeit attenuated, may be mediated by spliced isoforms lacking an α domain (*11*, *12*). The issue of the activity of single α-domain isoforms of NCLX is of particular physiological significance as these truncated NCLX isoforms, in contrast to NCX, are abundantly expressed in multiple tissues (*2*, *11*, *13*).

Subunits of ion channels and ion transporters form homo- or heterooligomers, providing the basis for functional diversity necessary for their physiological activity (*14*, *15*). In this study, applying a dominant-negative strategy for studying functional oligomerization, we sought to determine whether similar oligomerization of single α-domain NCLX exchangers (termed α1 and α2) may underlie the activity of these NCLX isoforms. Our results demonstrate that both α1 and α2 constructs are active and have distinct pharmacological and kinetic properties, among them sensitivity to the inhibitor, KB-R9743, and K^+ regulation. Importantly, a dominant-negative effect is exerted by a functional mutant, and a physical interaction between the single α-domain constructs is demonstrated by immunoprecipitation analysis. Thus, our results suggest that homo- or heterooligomerization is required for the single α-domain NCLX exchanger activity.

EXPERIMENTAL PROCEDURES

Construction of NCLX Mutants. Three NCLX constructs were generated, α1, α2, and α2-S273T. α1, corresponding to amino acids 1−439 of NCLX, was constructed by *Not*I digestion of the NCLXpCDNA3.1+ construct described previously (*3*). The resulting fragments were gel purified, and the long ∼6.7 kb fragment was religated. The ligation yielded a truncated NCLX construct lacking ∼400 bp coding for the last four C-terminal transmembrane domains, including the α2 region, and introducing two amino acid (RV) linkers and a new termination site coded by the vector sequence. α2 and α2-S273T, corresponding to amino acids 196−584 of NCLX, were constructed by using a polymerase chain reaction (PCR) based method. The α2 construct was generated using the following primers: a1 [forward, located at position 652 of the NCLX nucleotide sequence (accession no. AY601759)], TTCATGGCTGCCTCCAGGC, and a2 (reverse, located at position 1791), CATGCTTTTCAGGTGAATCACTCCAAATTC, designed to enhance the ∼1200 bp fragment corresponding to the 5′ end of NCLX ORF. For constructing the α2-S273T mutant, a second set of complementary primers was synthesized: b1 (forward, located at position 1457), TGGCCTGGGGGAACACAATTGGA, and b2 (the reverse complement of b1), TCCAATTGTTCCCCCAGGCCA. A conserved serine residue (located at position 468 in the NCLX polypeptide sequence) was changed to a threonine residue, and a unique *Mun*I site was introduced. Extensions coding for a 14 amino acid c-Myc epitope (CTAGGCCCCATTCAGATCCTCTTCTGAGATGAGTTTTTGTTC) or a 6His epitope (CTAGTGGTGGTGGTGGTGGTG) were added for the reverse primer of the first set introducing these tags at the C-terminal end of the constructs. Unique *Hin*dIII and *Xho*I restriction sites were inserted as extensions into the forward and reverse primers of the first set, respectively. For the α2-S273T construct, two PCR fragments were generated: (I) by using the forward primer from the first set and the reverse primer from the second and (II) by using the forward primer from the second set with the reverse primer (6His) from the first set. The purified PCR fragments were digested with *the Mun*I restriction enzyme and ligated into a pGEM-T (Promega) cloning vector. The α2 was constructed by using only the first set of primers (inserting a c-Myc epitope), and the PCR fragment was also ligated into the pGEM-T vector (Promega). The two constructs were excised with *Hin*dIII/*Xho*I and inserted into the *Hin*dIII/*Xho*I-digested pCDNA3.1+ vector (Invitrogen). All constructs were sequenced (Sequencing Unit, Biological Core Facility at the Institute for Applied Sciences at Ben-Gurion University). PCR was performed using the ExTaq PCR system (Takara). Plasmids were purified using the Hi-Speed plasmid purification kit (Qiagen) or GeneElute Hi-Speed midi kit (Sigma).

Cell Cultures and Plasmid Transfection. HEK293-T cells (human embryonic kidney cell line), PC-3 (prostate cancer cells), and HeLa cells (breast cancer cells) were cultured as described previously (*3*, *16*, *17*). Briefly, HEK293-T cells grown on glass coverslips were transfected with the indicated plasmid using standard calcium phosphate ($CaPO_4$) precipitation as previously described (*3*). The EYFP (0.35 μg) plasmid (Clontech) was added as a fluorescent reporter for the identification of transfected cells. Transport experiments or cell harvesting was carried out 25−35 h following transfection. For the electrophysiological experiments HEK293 cells were transfected using Ex-Gen 500 transfection reagent (Fermentas) according to manufacturer protocol. The pIRES CD8 plasmid (kindly provided by Prof. Bernard Attali, Tel Aviv University, Israel) was cotransfected with the indicated constructs or vector alone (at 1:4 ratio, respectively) for the identification of transfected cells as previously described (*18*). Cells were trypsinized and plated on glass coverslips precoated with poly-L-lysine (100 μM) 30 min prior to the electrophysiological experiments.

Fluorescent Measurements of Calcium Transport. The imaging system consisted of an Axiovert 100 inverted microscope (Zeiss), a Polychrome II monochromator (TILL Photonics, Planegg, Germany), and a SensiCam cooled charge-coupled device (PCO, Kelheim, Germany). Fluorescent imaging measurements were acquired with Imaging Workbench 2.2 (Axon Instruments, Foster City, CA).

Calcium Imaging. Cells were loaded for 30 min with 5 μM Fura-2 acetoxymethyl ester (AM; TEF-Lab, Austin, TX) in 0.1% BSA in Na^+ and Ca^{2+} containing Ringer's solution (120 mM NaCl, 5 mM KCl, 0.8 mM $MgCl_2$, 20 mM HEPES, 15 mM glucose, 1.8 mM $CaCl_2$, and 10 mM NaOH, buffered to pH 7.4). After dye loading, the cells were washed in Ringer's solution (20 min), and the coverslides were mounted in a perfusion chamber on a microscope stage. EYFP fluorescence (excitation using 480 nm and a 510 nm long-pass filter for the emission) was used to identify transfected cells, and then filters were switched to monitor Fura-2 fluorescence. Fura-2 was excited at 340 and 380 nm and imaged with a 510 nm long-pass filter; the results are presented as the ratio (*R*) between the emission signal

acquired using the two excitation wavelengths (340 nm/380 nm). Fluorescent ratio signals are normalized to the average signal obtained at the beginning of the measurements (R_0), thus allowing averaging of multiple experiments. Calcium influx assays were performed by perfusing the cells with Na^+-free Ringer's solution such that Na^+ was iso-osmotically replaced by NMG^+ (130 mM), with or without 5 mM KCl. Calcium efflux, in the "forward mode", was monitored by first loading the cells with Ca^{2+} by perfusion with the NMG^+ "reversal" medium and then switching to Na^+-containing Ringer's solution. Calcium efflux mediated by a Na^+/Ca^{2+} exchanger, acting in a forward mode, was also examined by determining the attenuation of Ca^{2+} influx via the store-operated channel as described before (*19*). Briefly, intracellular Ca^{2+} rise was induced by opening of the store-operated channel. Stores were depleted by the application of TG (200 nM thapsigargin; Alomone Labs, Jerusalem, Israel). Subsequently, Ca^{2+} (0.5 mM) was added in the presence or absence of Na^+, and the rate of intracellular Ca^{2+} change was determined. To determine the extent of SOC opening, cells were superfused with Ca^{2+}-free Ringer's solution containing 5 mM Mn^{2+} at the end of each experiment, and the rate of Fura-2 quenching was determined (360 nm excitation, 510 nm emission).

The results shown in all calcium imaging experiments are the average, ±SEM, of at least five independent experiments (n); in each experiment responses from at least 10 cells were acquired. Statistical analysis of the data was performed using the unpaired t-test and was calculated using Excel software.

Electrophysiological Recordings of $I_{Na/Ca}$. Whole cell recordings from HEK293 cells were performed in a physiological recording chamber (Warner Instruments) under a microscope (Olympus CKX41) essentially as described before (*20*). Patch microelectrodes with a tip of 3 μm diameter were pulled from capillary glass (A-M-Systems, no. 593200), using a Campden 753 microelectrode puller. The microelectrodes were filled with a solution containing 130 mM sodium glutamate, 20 mM NaCl, 20 mM tetraethylammonium chloride, 10 mM EGTA, and 20 mM Hepes (pH adjusted to 7.2 with Tris). Voltage clamp recordings were performed using an Axopatch-1D amplifier and digitized at 0.2 kHz with Axolab-1100. Cells were kept in a solution containing 150 mM NaCl, 5 mM KCl, 1.8 mM $CaCl_2$, 20 mM Hepes, and 10 mM glucose (pH adjusted to 7.4 with HCl). After a gigaohm seal was formed, the cells were superfused with a solution containing 130 mM NMDG, 10 mM sucrose, 1 mM EDTA, and 20 mM Hepes (pH adjusted to 7.4 with HCl), and baseline currents were recorded with cells held at $V_m = 0$ mV. Reverse Na^+/Ca^{2+} exchange currents were measured following the addition of 0.2 mM Ca^{2+} (without EDTA), and then Ca^{2+} was removed by adding 5 mM EDTA. Data were analyzed off line using PCLAMP software (Axon Instruments); averaging was done in groups 10 data points using Matlab software (by Math-Works).

Immunoblot and Immunoprecipitation. HEK293-T cells expressing the different NCLX constructs or control were washed once with ice-cold PBS solution, scraped from the plate using a rubber policeman, and placed into RIPA buffer. Total protein was quantified by the Bradford dye-binding procedure (Bio-Rad). Protein expression was resolved by SDS−PAGE and transferred onto nitrocellulose membranes. Immunoblot analysis was carried out as previously described (*21*), using an antibody targeted against c-Myc epitope (Santa Cruz) at 1/500 dilution or the NCLX antiserum (*3*) at a 1/2500 dilution under reducing and nonreducing conditions without β-mercaptoethanol. The immunoprecipitation procedure was performed using the ExactaCruz set (Santa Cruz Biotechnology) according to manufacturer protocol. Briefly, total cell lysate from HEK293-T cells expressing the α2 (expressing the c-Myc tag), α2-S273T (expressing the 6His tag), or both was incubated with 20 μg of an antibody targeted against the 6His epitope (Santa Cruz) overnight at 4 °C. Subsequently 50 μL of the IP matrix was added to the lysate, and beads were then sedimented and further processed according to manufacturer instructions.

Analysis of Protein Surface Expression. Surface expression of the various constructs was determined using the experimental approach recently described by Kim et al. (*22*). Briefly, control, α2, or α2-S273T expressing cells grown on glass coverslips were fixed with 4% paraformaldehyde in PBS solution for 30 min and washed three times with PBS (pH 7.4) (*23*). Fixed cells were blocked with normal goat serum without permeabilizing agents and then incubated overnight at 4−8 °C with antibodies against the c-Myc epitope (1:1000) (Santa Cruz) for α2 labeling or the 6His epitope (1:200) for α2-S273T labeling. Cells were washed with PBS (×3) and incubated with Cy2-conjugated anti-rabbit IgG for 1 h at room temperature. After being rinsed with PBS, the coverslips were mounted with Immu-mount (Shandon), and images were acquired using a Zeiss LSM510 confocal microscope.

RESULTS

Na^+/Ca^{2+} Exchange Mediated by NCLX α1 and α2 Constructs. We first assessed the activity of the short NCLX exchanger molecules lacking either α1 or α2 repeat domains. For this purpose, we generated two different constructs of NCLX (Figure 1a): α1 corresponding to amino acids 1−439 and, therefore, lacking the α2 domain; and α2 corresponding to amino acids 196−584, in which the α1 domain is completely truncated. The activity of these constructs was determined by monitoring fluorescence changes following intracellular Ca^{2+} changes under reversal (Na^+ free, NMG^+ iso-osmotically substituting for Na^+) and forward (Na^+ Ringer's) exchange modes in HEK293-T cells heterologously expressing the α1 or α2 constructs as previously done for the full-length NCLX (*3*). The removal of Na^+ was followed by robust increase in Ca^{2+} influx in cells expressing either constructs but not in control cells (Figure 1b). The subsequent addition of Na^+ induced a decrease in $[Ca^{2+}]_i$, for either α1 or α2 constructs, that was again absent in control cells. Transport activity was monitored for both constructs, albeit the Ca^{2+} influx rate was approximately 30% lower for the α1 compared to the α2 construct. Immunoblot analysis of HEK293-T cell extracts indicated that transfection by both constructs yielded a similar protein expression level (see Figure 6). Similar exchange activity was also monitored in PC-3 and HeLa cells transfected by α1 or α2, respectively (not shown).

To compare between the activity of the α1 and α2 constructs and the full-length NCLX and to further assess their Ca^{2+} efflux activity, we determined, in HEK293-T cells, the intracellular Ca^{2+} rise following opening of SOC trig-

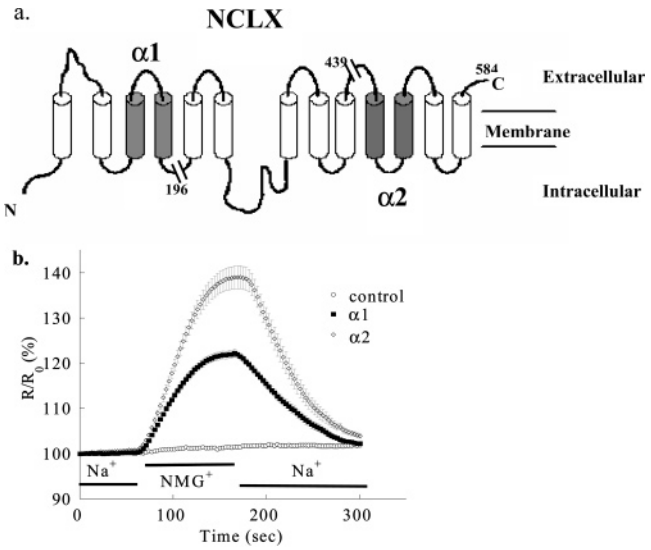

FIGURE 1: Putative structure and activity of the α1 and α2 single-domain constructs. (a) The putative transmembrane topology model of NCLX is depicted using TopPred (*2*, *40*). Cylinders represent the transmembrane domains. The putative α-repeat regions are colored in gray. The α1 and α2 constructs are delineated (1−439 and 196−584, respectively). (b) HEK293-T cells transfected with either α1 ($n = 5$), α2 ($n = 5$), or vector alone (control, $n = 5$) plasmids were loaded with Fura-2 and superfused with the indicated Ringer's solution. Transport of Ca^{2+} in the reversal and forward modes was monitored in cells expressing either α1 or α2.

gered by the depletion of the stores using TG (see Experimental Procedures). This Ca^{2+} rise can be attenuated by Ca^{2+} efflux mediated by a Na^+/Ca^{2+} exchanger acting in the forward mode as previously described (*24*). Application of TG in Ca^{2+}-free Ringer's solution triggered an intracellular Ca^{2+} rise, originating from intracellular stores, that was followed by a decline to a steady state. This decline was about 3-fold faster in the single α-domain-expressing cells compared to vector-transfected cells, in the presence of Na^+ (see Figure 2a). Following opening of the SOC and addition of 0.5 mM Ca^{2+}, the rate of intracellular Ca^{2+} rise was determined in cells expressing the various NCLX constructs and compared with vector-transfected cells in the presence or absence of Na^+ (see Experimental Procedures and Figure 2). As shown, rates of Ca^{2+} rise in the presence of Na^+ were significantly lower in cells expressing NCLX, α1, or α2 versus the control cells (Figure 2b). In the absence of Na^+ (Figure 2c), however, the rate of Ca^{2+} rise in cells expressing the NCLX constructs was higher, and no significant change is observed compared to the control cells. To determine if the changes in Ca^{2+} influx rates observed in the cells expressing the NCLX constructs were not triggered nonspecifically by changes in SOC activity, we determined the rates of Mn^{2+} influx via this pathway. The latter cation freely permeates through the SOC but is not transported by NCLX (Palty et al., unpublished results). As shown in Figure 2d, rates of Mn^{2+} permeation were slightly higher in cells expressing NCLX or the single α-domain constructs versus vector-transfected cells, indicating that the attenuation of Ca^{2+} influx cannot be attributed to a decrease in SOC activity.

To ascertain that the α1 and α2 constructs mediate Na^+/Ca^{2+} exchange, electrophysiological measurements were performed using whole cell patch configuration using the

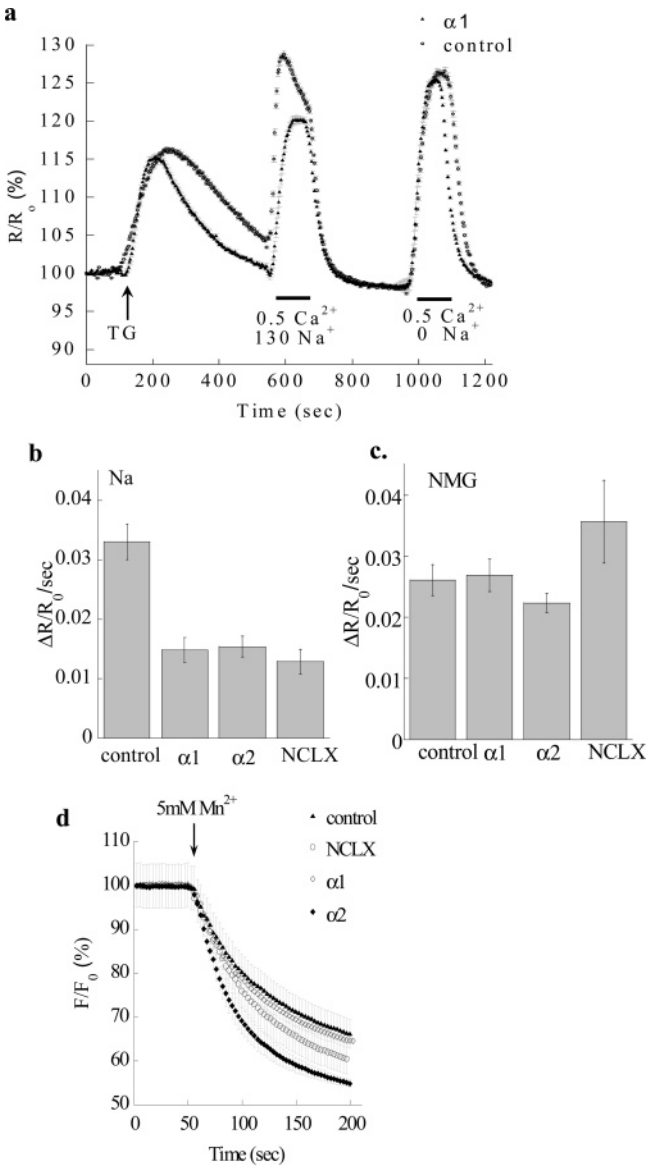

FIGURE 2: Net intracellular Ca^{2+} rise mediated through the store-operated channels (SOC) in cells expressing the NCLX constructs. (a) The experimental paradigm. Cells were treated with 0.2 μM TG in Na^+-containing Ca^{2+}-free Ringer's solution; subsequently 0.5 mM Ca^{2+} was added in the presence or absence of Na^+ (NMG^+ replacing Na^+ in Ringer's solution) as indicated by the bar beneath the graph, followed by superfusion with Ca^{2+}-free Ringer's solution to allow the rapid removal of Ca^{2+}. (b) Rates of Ca^{2+} rise in the presence of Na^+ in cells expressing NCLX ($n = 8$), α1 ($n = 10$), or α2 ($n = 10$) versus vector-transfected cells ($n = 10$). (c) Rates of Ca^{2+} rise in the absence of Na^+ in cells expressing NCLX, α1, or α2 versus vector-transfected cells. (d) To assess SOC permeability, independent of Na^+/Ca^{2+} exchange, 5 mM Mn^{2+} was applied in Ca^{2+}-free Ringer's solution, and the rate of Fura-2 fluorescence quenching was determined.

experimental paradigm previously described for NCKX2 (*20*). Cells were cotransfected with α1 or α2 constructs and with a pIRES CD8 plasmid, used to identify transfected cells. As shown in Figure 3, bath application of Ca^{2+} (0.2 mM), in the absence of Na^+, elicited outward currents (reverse exchange) in α1 or α2 transfected cells. Reverse exchange outward currents recorded for α1 and α2 were 11.8 ± 3.5 ($n = 9$) and 11.3 ± 3.0 pA ($n = 6$), respectively, and were similar in magnitude to currents previously recorded for NCKX2 and NCKX3 (*20*, *25*). A current of similar magni-

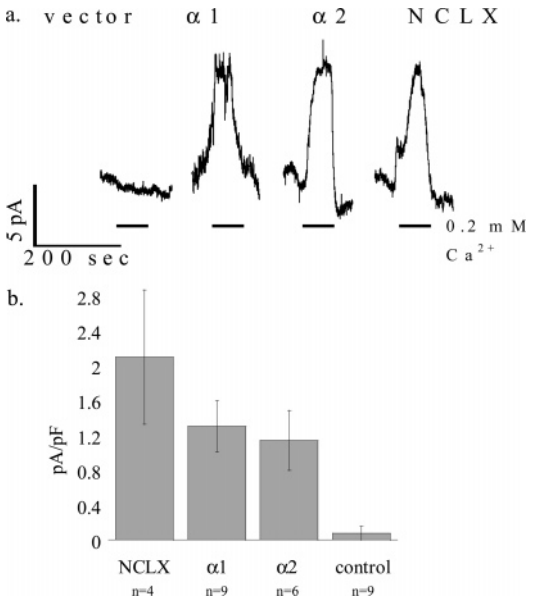

FIGURE 3: Electrophysiological measurements of the activity mediated by the α1 and α2 single-domain constructs. (a) Whole cell patch clamp analysis of the cells expressing α1 or α2. The outward currents were induced by bath application of Ca^{2+} (0.2 mM) in the absence of Na^+ at a holding potential of 0 mV. Representative currents recorded from cells expressing NCLX, the α2 or α1 constructs, and vector (control) are shown. (b) Averaged current densities of reverse $I_{Na/Ca}$ were normalized according to membrane capacitance. n = number of cells in each experiment.

tude was also recorded in cells expressing the full-length NCLX; curiously and for unknown reasons, it was more difficult to obtain a proper seal in the NCLX-expressing cells, and once a seal was formed, it was less stable. No current (0.4 ± 0.4 pA; $n = 9$) was monitored in control cells. Our results, thus, indicate that constructs lacking either one of the catalytic α-repeat domains may mediate electrogenic Na^+/Ca^{2+} exchange.

Effect of External K^+ or Li^+ Ions and the KB-R7943 Compound on Activity of NCLX Constructs. To determine the K^+ dependence of α1 and α2, we applied the paradigm described in Figure 1 in the absence or presence of 5 mM K^+. If Na^+/Ca^{2+} exchange mediated by one of our constructs is K^+-dependent, a robust reduction in Ca^{2+} influx rate or amplitude would be expected in the absence of K^+. As shown in Figure 4, rates of Ca^{2+} transport were approximately 30% higher for the α1 construct in the presence of 5 mM K^+ compared to its absence (Figure 4a), while Ca^{2+} exchange rates for the α2 construct are not altered in the presence or absence of 5 mM K^+ (Figure 4b). The similar effect of K^+ on the reversal and efflux mode of the α1 construct indicates that it is not related to the change in membrane potential mediated by the application of K^+ nor that this ion is transported by this construct. The isothiourea compound, KB-R7943, is a potent inhibitor of NCX, which was suggested to interact with residues in the α2 domain of NCX1 and NCX3 (*26*). We have previously demonstrated that KB-R7943 also acts as a partial inhibitor of NCLX, with an IC_{50} of ~10 μM, compared to ~5 μM for NCX1 (*27*). The activity of single α-domain constructs offered us the opportunity to determine whether the inhibitor interacts with one of the single-domain constructs of NCLX. As shown in Figure 4c, a partial inhibition (~50%) of the α1 activity was observed following application of 5 μM KB-R7943. No further inhibition was monitored while applying higher concentrations of this inhibitor, indicating that, similarly to the effect on the full-length NCLX (*3*), KB-R7943 acts as a partial inhibitor of the α1 construct. In contrast, application of KB-R7943 had almost no inhibitory effect on the activity of the α2 construct, even when used at higher concentrations (up to 20 μM). Our results hence indicate that KB-R7943 interacts with the α1 but not with the α2 domain of NCLX.

To determine the Li^+ selectivity of α1 and α2 constructs, rates of Ca^{2+} efflux were compared in the presence of Na^+, NMG^+, or Li^+. As shown in Figure 4d,e, in cells expressing either the α1 or α2 construct, similar Ca^{2+} efflux rates were detected in the presence of Na^+ or Li^+, while the Ca^{2+} efflux rates in the presence of NMG^+, for each of the constructs, were about 10-fold lower. Our results, therefore, indicate that the Na^+/Ca^{2+} exchange mediated by the NCLX constructs is not K^+-dependent, but this ion may have a regulatory effect on the rate of Na^+/Ca^{2+} exchange mediated by the α1 construct. Yet, both α1 and α2 constructs retain the unique Li^+ selectivity of the full-length NCLX.

Activity Expression and Surface Expression of the α2 and α2-S273T Mutant. The results described above indicate that both the α1 and α2 constructs mediate, individually, Na^+/Ca^{2+} exchange. To test the hypothesis that oligomerization of the single-domain proteins is required for Na^+/Ca^{2+} exchange activity, we applied the dominant-negative approach of coexpressing the functional α1 or α2 constructs together with a nonfunctional NCLX. We generated a mutant of the α2 construct by replacing a serine residue at position 468 of NCLX with threonine (α2-S273T). This residue was chosen because it is highly conserved among NCX and NCKX and is essential for both NCX1 and NCKX2 activity (*6*, *28*). As shown in Figure 5a, there was no apparent Ca^{2+} transport in cells expressing the α2-S273T, in the reverse or efflux mode, indicating that also in NCLX this conserved residue is required for cation transport. Using the whole cell patch paradigm described in Figure 3, we did not detect significant reverse exchange currents in cells expressing the α2-S273T mutant (2 ± 1 pA, $n = 5$, Figure 5b). Thus the fluorescence and electrophysiological analysis indicate that the α2-S273T is inactive. To further determine if the mutant is sorted properly into the plasma membrane and does not interfere with sorting of the α2 construct, we determined the surface expression of the constructs in nonpermeabilized cells (see Experimental Procedures). For this purpose, c-Myc and 6His tags were inserted at the C-terminal domain of the constructs (see Figure 1), and transfected cells were immunocytochemically stained. As shown in Figure 5c, the fluorescent stain was localized to the plasma membrane. Furthermore, no reduction of immunoreactive c-Myc, corresponding to α2 expression, was observed when cells were cotransfected with equal amounts of α2 and α2-S273T plasmid constructs (Figure 5d). No labeling was, however, observed in control (vector-transfected) cells, suggesting that the staining can be attributed to surface expression of the constructs. To determine if the α2-S273T mutant interferes with expression of the WT α2, cells were transfected with the α2 (tagged with c-Myc) or cotransfected with both α2 and α2-S273T (tagged with 6His). Subsequently, the expression of the c-Myc-tagged α2 was assessed by immunoblot analysis using an antibody for the c-Myc tag. As shown in

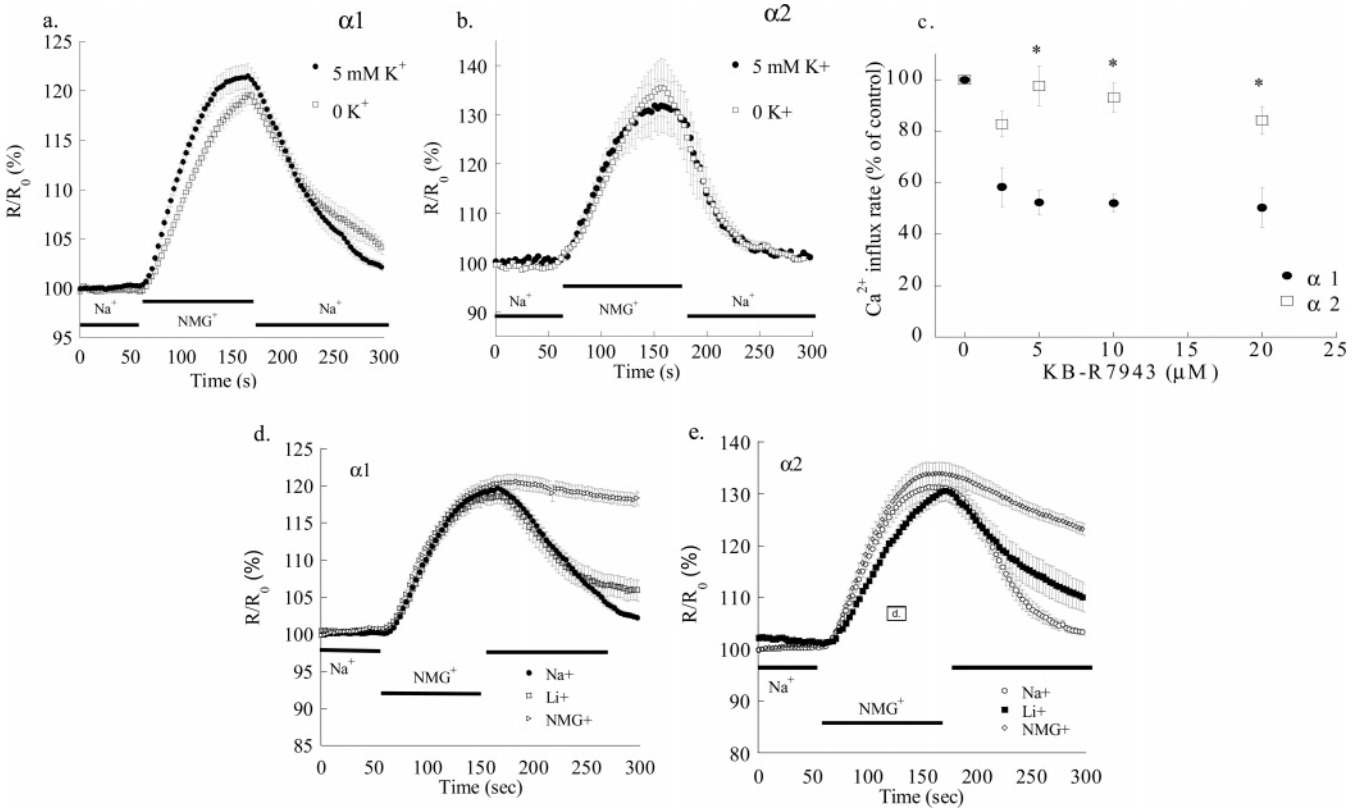

FIGURE 4: Role of K^+ or Li^+ ions and inhibition by KB-R7943 on Na^+/Ca^{2+} exchange mediated by the α1 and α2 constructs. The same experimental paradigm shown in Figure 1 was employed, using either K^+-free or 5 mM K^+-containing Ringer's solution. (a) Activity mediated by the α1 construct ($n = 5$) is ~30% higher in the presence of 5 mM K^+. (b) Activity mediated by the α2 construct ($n = 5$) was not affected by the presence of K^+. (c) Initial rates of Ca^{2+} influx were measured in the presence of the indicated concentration of KB-R7943, in cells expressing either α1 ($n = 6$) or α2 ($n = 6$) constructs, using the reversal paradigm in which Na^+ is substituted by NMG^+ in Ringer's solution (* = $P < 0.05$). Application of KB-R7943 resulted in ~50% inhibition of the α1 construct activity, whereas no significant inhibition was apparent in cells expressing the α2 construct. The same experimental paradigm shown in Figure 1 was employed in cells expressing the α1 ($n = 5$) (d) or α2 ($n = 5$) (e); following Ca^{2+} loading of cells by activation of the reversal mode, cells were superfused with either Na^+, Li^+, or NMG^+ containing Ringer's solution, and Ca^{2+} efflux was monitored.

Figure 5e a polypeptide of ~50 kDa (marked by an arrow) was stained at similar intensity in extracts of α2 and α2-S273T + α2 transfected cells but not in vector or α2-S273T transfected cells. Similar staining of higher and lower molecular mass polypeptides that was also apparent in vector and α2-S273T samples is probably related to interaction of the c-Myc antibody with endogenous HEK proteins (*29*). Hence our results indicate that the α2-S273T protein is properly sorted into the plasma membrane and that it does not interfere with the expression and the plasma membrane sorting of the α2 protein.

Immunoblot and Immunoprecipitation Analysis of Complex Formation by the Single-Domain Constructs. To determine the expression levels and the molecular masses of the polypeptides derived from the constructs, transfection with the mono-α constructs and immunoblot analysis were performed using the NCLX antibody that was generated against an epitope shared by both constructs (*3*). As shown in Figure 6a, the expression level of the constructs was similar. No staining of the vector-transfected cell was apparent, indicating that the antibody specifically recognized the constructs. The small differences in the molecular mass of the α2 and α2-S273T constructs are probably caused by the 6His and c-Myc tagging. Interestingly, however, an additional polypeptide of ~75 kDa, a molecular mass corresponding in size to a dimeric form, was apparent for the α1 construct. To address this issue further, the same immunoblot analysis was conducted under nonreducing conditions by omitting *β*-mercaptoethanol from the samples. As shown in Figure 6b under nonreducing conditions, conversion of the lower mass α1 band to the higher ~75 kDa form was also apparent. A lower ~15 kDa polypeptide, probably a proteolytic fragment, was also apparent for the α2 line. Altogether, the immunoblot analyses suggest that the α1 and α2 constructs are found in a molecular mass which may correspond to a monomer and in a higher molecular mass which potentially corresponds to a dimer. The latter form is apparent primarily under nonreducing conditions. To directly demonstrate interaction between the single α-domain constructs, we performed an immunoprecipitation analysis. Cells were cotransfected with the α2 construct tagged by c-Myc and the α2-S273T construct tagged with 6His. Cells were lysed, reacted, and pulled down with the 6His antibody (see Experimental Procedures). Immunoblot analysis of the 6His pull-down extract using the c-Myc or NCLX antibodies revealed a band at approximately 50 kDa (Figure 6c,d). The above results suggest that the α2 construct interacts to form an oligomeric structure.

Oligomerization of the α1 and α2 Constructs. If the single α-domain constructs are functionally interacting through an oligomer complex, adding a nonfunctional subunit would

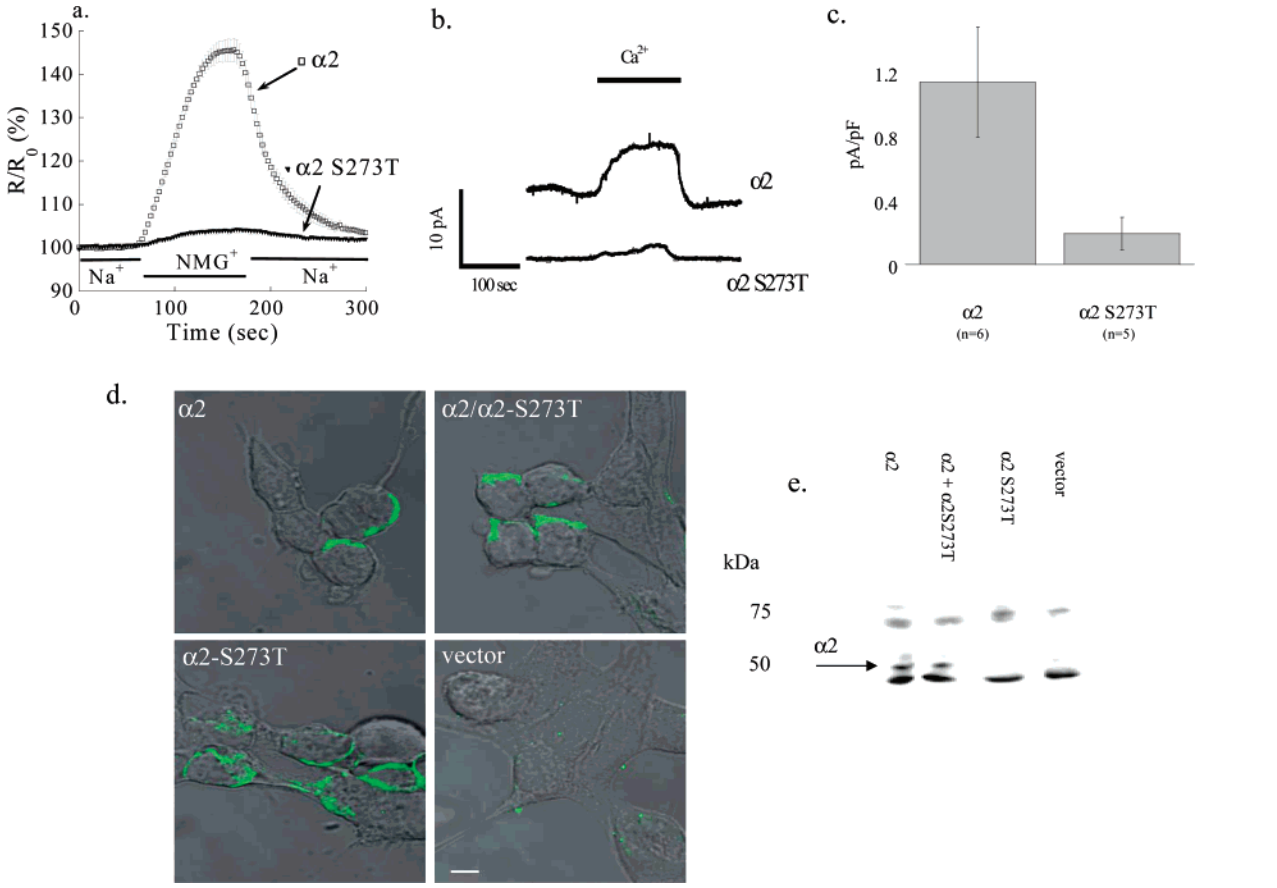

FIGURE 5: Activity and surface expression of the α2-S273T mutant. HEK293-T cells were transfected with the α2 construct tagged with c-Myc or the α2-S273T construct tagged with 6His epitope. (a) Na^+/Ca^{2+} exchange was monitored using the paradigm described in Figure 1. No Ca^{2+} transport activity was observed in cells expressing the α2-S273T, indicating that the mutant is inactive. (b) Representative recording of reverse $I_{Na/Ca}$ taken from HEK293 cells transfected with the α2-S273T construct. The same recording trace as in Figure 2 of a cell expressing the α2 construct is shown for comparison. The bar graph depicts the averaged current densities of reverse $I_{Na/Ca}$ recorded from cells expressing the α2-S273T normalized according to membrane capacitance and compared to those of the WT α2. (c) Surface expression was monitored by immunostaining of nonpermeabilized cells (see Experimental Procedures) transfected with each construct or coexpressing the α2 and the α2-S273T (1:1) constructs. Antibodies against c-Myc were used for α2 staining in the cells transfected with the α2 or both α2/α2-S273T constructs and for the vector-transfected cells. Antibodies against 6His were used for the detection in the α2-S273T-transfected cells. Confocal images from a single optical section are shown projected on the transmitted light images of the cells. Surface expression is observed following the transfection with the α2, α2-S273T, or α2/α2-S273T plasmids. The scale bar is 5 μm for all images. (e) Immunoblot analysis of the α2 c-Myc-tagged construct. Extracts of cells transfected with either the α2 (c-Myc tagged), α2-S273T (6His tagged), both plasmids, or vector alone were subjected to immunoblot analysis with c-Myc antibody. The arrow marks the position of the α2. Note that the apparent expression of α2 is unaltered by the coexpression of the α2-S273T mutant.

have a dominant-negative effect on the oligomer activity. A prerequisite for using the dominant-negative approach is that the activity will linearly correlate with plasmid concentration and that the expression of the mutant will not change the expression of the WT construct. The activity of the α2 construct as a function of plasmid concentration was linear between amounts of plasmid ranging from 2 to 8 μg. To assess the number of subunits required for the exchanger functional unit, we carried out an inhibitory dose−response analysis. This was performed by monitoring Ca^{2+} transport in cells coexpressing the α2 construct (2 μg) with increasing amounts of the α2-S273T mutant, thus keeping the total amount of plasmid in the linear range. Such strategy has been successfully used for analyzing the number of interacting subunits in both channels and transporters (*30*, *31*). As shown in Figure 7a,b, increasing the amount of α2-S273T plasmid resulted in a dose-dependent decrease in Ca^{2+} transport, leading to approximately 70% inhibition of the initial activity in the presence of 1.6 μg of α2-S273T plasmid. We then used the inhibition curve to predict the functional unit number required for the α2 activity. This analysis assumes that in the presence of one inactive monomer the oligomer is inactivated (*30*, *32*), leading to a binomial distribution reflecting the activity of the oligomer. To calculate the number of subunits required, the fractional activity of the oligomer was plotted against the fractional amount of the active α2 construct (α2/α2 + α2-S273T) (*30*). For comparison, the graph also shows the predicted curves for the dimeric and tetrameric structures (Figure 7b). Fitting the inhibition curve indicated that the functional unit is most likely a dimer ($n = 2.3 \pm 0.2$). We subsequently sought to determine if the α2-S273T expression will also affect the activity of the α1 construct. About 3-fold inhibition of the activity was observed when the α1 and α2-S273T were coexpressed (Figure 7d). Taken together, the α2-S273T construct had a dominant-negative effect upon coexpression with α1 or α2. Our results, therefore, indicate that both α1 and α2 domains are capable of forming hetero- or homooligomers.

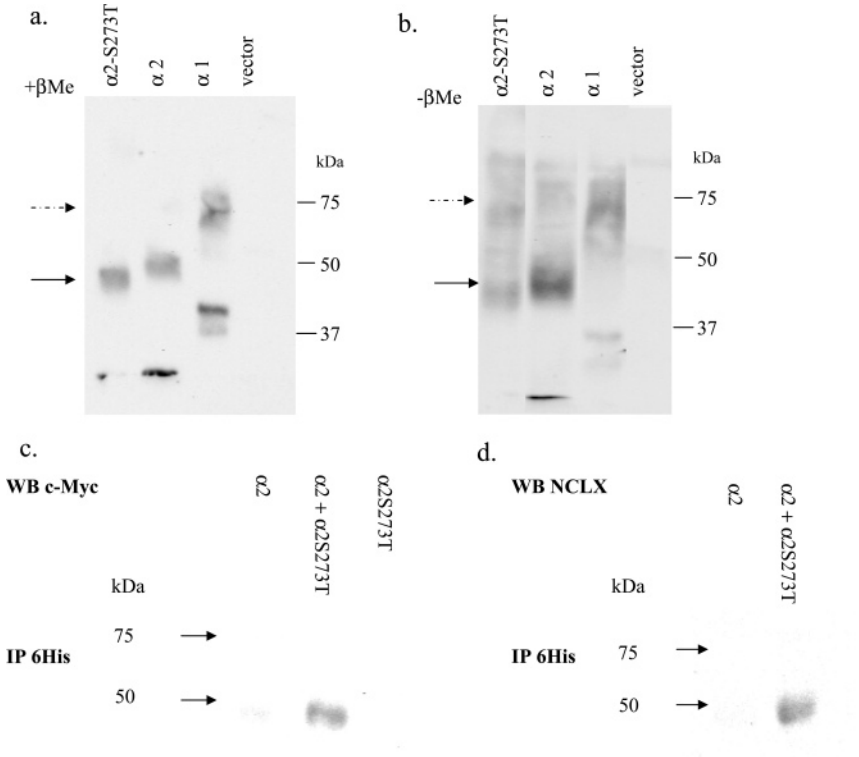

FIGURE 6: Immunoblot analysis of the single-domain constructs under reducing and nonreducing conditions and immunoprecipitation analysis of α2 and α2-S273T complex formation. Immunoblot analysis using an NCLX antibody was conducted on HEK293-T cell extracts (20 μg) expressing the indicated constructs in the presence (a) or absence (b) of β-mercaptoethanol. Arrows point to the lower (solid arrow) and higher (dashed arrow) molecular weight forms of the expressed constructs. (c, d) Immunoprecipitation analysis of the α2 and α2-S273T interaction. Lysates of cells transfected with the α2 or the α2-S273 or cotransfected with both (α2-c-Myc and α2-S273T-6His) were immunoprecipitated with the 6His antibody, and immunoblot analysis was performed with antibodies against c-Myc (c) or NCLX (d) as described under Experimental Procedures.

DISCUSSION

It has been recently demonstrated that spliced isoforms of NCLX, partially truncated at either the α1 (*3*) or α2 (*2*), are capable of mediating cation transport. It was not clear, however, if the partially truncated α-repeat was necessary for cation transport or whether the other, intact repeat was sufficient. To address this, we have generated artificial NCLX constructs in which either the α1 or α2 constructs were completely removed. The following results strongly indicate that both the α1 and α2 constructs mediate Na^+/Ca^{2+} exchange: (1) fluorescence analysis of Ca^{2+} transport in cells expressing the α1 and α2 shows that the expression of these single-domain constructs is followed by robust Na^+-dependent Ca^{2+} transport in both the reversal and efflux modes; (2) electrophysiological measurements in HEK293 cells expressing the α1 and α2 constructs show reverse Na^+/Ca^{2+} exchange current that is absent in control cells; (3) a mutation of a conserved serine (position 468 on the NCLX polypeptide) inactivates Na^+/Ca^{2+} exchange, Ca^{2+} transport, and current.

Importantly, both single-domain constructs of NCLX exhibit Na^+/Ca^{2+} exchange activity; furthermore, their Ca^{2+}-induced currents are also similar to those previously monitored for NCKX (*20*, *25*). The fact that their activity was monitored in remotely related cell lines, HEK293 (embryonic kidney) and PC-3 (prostate metastatic), as well as HeLa (breast cancer) cells, indicates that the transport mediated by the constructs is not restricted to a specific cell type. Our results further indicate that oligomerization is essential for the activity of the single α-domain constructs. A striking dominant-negative effect of the mutated construct, on both active single α-domain constructs, suggests that the functional basis for single NCLX α-domain protein activity relies on subunit oligomerization. The similar expression level of the α2 construct in the presence of α2-S273T argues against a nonspecific effect of the mutant. Analysis of the inhibitory effect of the dominant-negative construct indicates that the functional unit is an oligomer composed of either two or three subunits. Although the quantitative analysis does not enable to strictly distinguish between a trimer and a dimer, the latter seems more reasonable. This is based on the fact that the best fit of the data is for a dimer ($n = 2.3 \pm 0.2$) and that the higher molecular mass forms of both α1 and α2, which are particularly apparent under nonreducing conditions, are similar in size to a dimer. The functional data are supported by immunoprecipitation analysis which shows that the single α2 construct and the functional α2 mutant physically interact. Hence our results support the assertion that each α-domain of NCLX contains all of the necessary elements for Na^+/Ca^{2+} exchange activity, while oligomerization is essential for the transport activity. Such functional organization may have important implications for the physiological diversity of activity and regulation of single α-domain spliced Na^+/Ca^{2+} isoforms naturally found in different tissues.

The full-length NCLX protein has been shown by us to mediate K^+-independent Na^+/Ca^{2+} exchange (*3*). Furthermore, we have shown that a human splice variant of NCLX, s-NCLX, catalyzes K^+-independent Na^+/Ca^{2+} and Li^+/Ca^{2+}

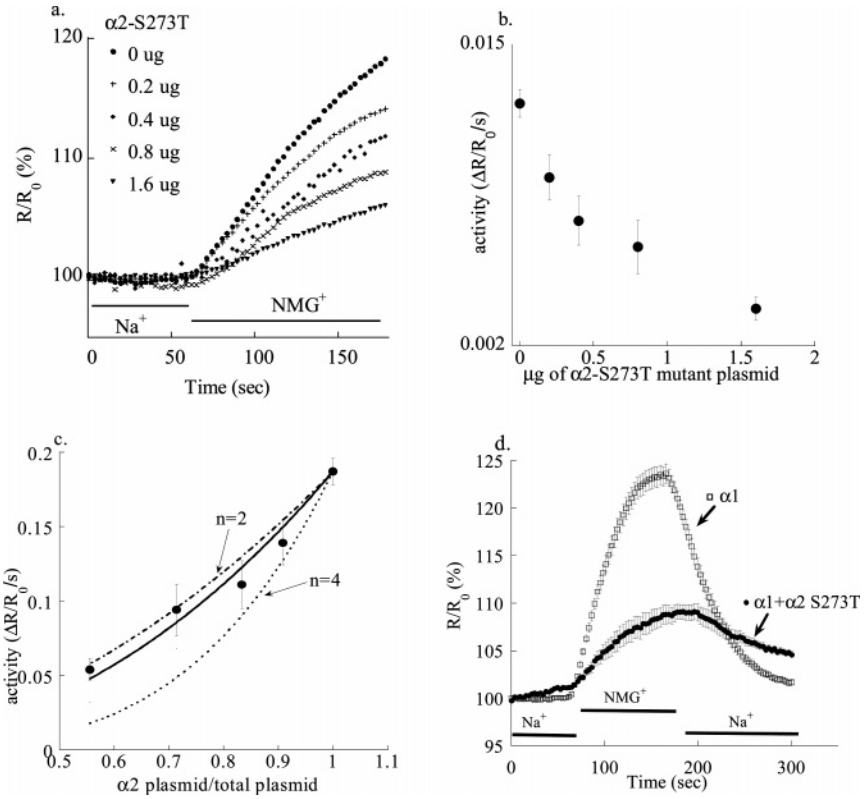

FIGURE 7: Dose-dependent inhibition of Na^+/Ca^{2+} exchange by the α2-S273T mutant. (a) Cells were cotransfected with 2 μg of the α2 plasmid and α2-S273T plasmid at the indicated amounts ($n = 6$ for all experiments). The rate of Na^+/Ca^{2+} exchange was monitored in the reversal mode. The exchange activity observed at the various amounts of α2-S273T is shown. (b) The rates of Ca^{2+} influx was determined from (a), $\Delta(R/R_0)/S$, and is plotted versus the amount of α2-S273T. (c) The same data (b) were analyzed by presenting the fractional amount of the constructs (α2/α2 + α2-S273T) versus the activity [$\Delta(R/R_0)$/15 s]. The points are fitted (solid line) using an equation which assumes a binomial distribution as previously described (*30*, *32*): activity $= F_{\alpha 2}{}^n V_{\alpha 2}$, where $F_{\alpha 2}$ is the fractional amount of α2, n is the stoichiometry of the subunit number, and $V_{\alpha 2}$ is the activity of α2 at the absence of α2-S273T. This analysis yielded a value of 2.3 ± 0.2 for n. The dotted lines are the predicted curves for a dimer ($n = 2$) and a tetramer ($n = 4$). (d) Ca^{2+} transport was monitored in cells cotransfected with 4 μg of the indicated constructs. Coexpression of the α2-S273T construct with α1 inhibited the Na^+/Ca^{2+} exchange activity.

exchange, despite a large truncation of key residues from the α1 catalytic domain. An earlier study has identified a mouse spliced isoform (s-Mu) which is also truncated, but at the α2 domain, and suggested that it is a K^+-dependent Na^+/Ca^{2+} exchanger which is inert to Li^+ (*2*). Considering the functional oligomerization of the single α-domain proteins, the s-Mu activity may result if the α1 domain specifically catalyzes K^+-dependent Na^+/Ca^{2+} exchange. The reactivity of both single α-domain constructs with Li^+ and the modest noncatalytic effect of K^+ monitored in this work, however, argue against this hypothesis. Our results further indicate that KB-R7943 acts as a partial though potent inhibitor of the α1 construct while no inhibitory effect is monitored on the α2 construct. Interestingly, the partial though high-affinity KB-R7943 inhibition is similar for the full-length NCLX and the α1 construct, suggesting that the KB-R7943 inhibitory site resides on the latter construct.

The molecular basis for the single-domain activity of NCLX is not, at present, clear. It is worth noting that the intramolecular regions of homology of the Na^+/Ca^{2+} exchangers have been suggested to originate from an early gene duplication event (*33*). Recently, the evolution of the cation/Ca^{2+} exchanger family has been analyzed (*34*), with the results suggesting that NCLX forms a unique group, branching early in the evolutionary tree of this family of transporters. Hence, an intriguing possibility is that NCLX retains at least some ancestral flexibility of a single α-domain protein catalyzing ion transport. Thus it is tempting to speculate that this functional−structural flexibility may have been largely lost in the more recent NCX members. This may explain the lower or complete lack of activity of a single α-domain isoform of NCX1, compared to the activity of the single-domain, truncated, NCLX construct or its naturally occurring single-domain isoforms.

Previous topological models of NCX, although not confirmed by a three-dimensional structural analysis, have suggested that the two α-domains face opposite directions, i.e., α1 facing the extracellular and α2 the intracellular side of the plasma membrane in a so-called "hourglass" model (*35*). We do not know, at present, the topological arrangement of the full-length NCLX or of the single α-domain, functional, oligomers. Yet, for the homodimer proteins to follow the predicted hourglass model will require that the single α-domain proteins will have a dual topology, namely, that these monomers will be inserted in opposing orientations into the membrane. This seemingly unlikely configuration was recently demonstrated in a three-dimensional crystal structure of the homodimeric bacterial H^+/drug exchanger, EmrE, in which the homomonomeric proteins interact in an antiparallel configuration that is slightly asymmetrical (*36*). Such unique membrane organization has been also proposed on the basis of topological screening for several other

membrane proteins (*37*, *38*). We therefore propose that an antiparallel configuration of the single α-domain proteins may consist of the simplest model reconciling the hourglass organization of the NCX with the functional homodimerization of NCLX suggested in this study. Alternatively, the two α-domains may be arranged at a similar membrane orientation, a configuration that is common in cation channels (*39*). Future topological studies are required to distinguish between these two modes of membrane organizations.

Finally, the remarkable structural flexibility of single α-domain isoforms of the NCLX demonstrated in this study suggests that they may similarly interact with other members of the Na^+/Ca^{2+} exchanger superfamily. Because these splice isoforms of NCLX are coexpressed in tissues with other members abundantly expressed, such interaction may extend and diversify the activity and regulation of Na^+/Ca^{2+} exchangers in multiple tissues.

ACKNOWLEDGMENT

We thank Drs. Ze'ev Silverman and Ofer Yifrach for critical reading and helpful discussions throughout the preparation of the manuscript and Dr. Bernard Attali for invaluable help in establishing the electrophysiological setup.

REFERENCES

1. Blaustein, M. P., and Lederer, W. J. (1999) Sodium/calcium exchange: its physiological implications, *Physiol. Rev. 79*, 763−854.
2. Cai, X., and Lytton, J. (2004) Molecular cloning of a sixth member of the K^+-dependent Na^+/Ca^{2+} exchanger gene family, NCKX6, *J. Biol. Chem. 279*, 5867−5876.
3. Palty, R., Ohana, E., Hershfinkel, M., Volokita, M., Elgazar, V., Beharier, O., Silverman, W. F., Argaman, M., and Sekler, I. (2004) Lithium-calcium exchange is mediated by a distinct potassium-independent sodium-calcium exchanger, *J. Biol. Chem. 279*, 25234−25240.
4. Schneider, J. W., Mercer, R. W., Gilmore-Herbert, M., Utset, M. F., Lai, C., Greene, A., and Benzer, E. (1988) Tissue specificity localization in brain and cell-free translation of mRNA encoding the A3 isoform of (Na + K^+)-ATPase, *Proc. Natl. Acad. Sci. U.S.A. 85*, 284−288.
5. Schulze, D. H., Polumuri, S. K., Gille, T., and Ruknudin, A. (2002) Functional regulation of alternatively spliced Na^+/Ca^{2+} exchanger (NCX1) isoforms, *Ann. N.Y. Acad. Sci. 976*, 187−196.
6. Winkfein, R. J., Szerencsei, R. T., Kinjo, T. G., Kang, K., Perizzolo, M., Eisner, L., and Schnetkamp, P. P. (2003) Scanning mutagenesis of the alpha repeats and of the transmembrane acidic residues of the human retinal cone Na/Ca-K exchanger, *Biochemistry 42*, 543−552.
7. Kinjo, T. G., Szerencsei, R. T., Winkfein, R. J., Kang, K., and Schnetkamp, P. P. (2003) Topology of the retinal cone NCKX2 Na/Ca-K exchanger, *Biochemistry 42*, 2485−2491.
8. Shigekawa, M., Iwamoto, T., Uehara, A., and Kita, S. (2002) Probing ion binding sites in the Na^+/Ca^{2+} exchanger, *Ann. N.Y. Acad. Sci. 976*, 19−30.
9. Ottolia, M., John, S., Qiu, Z., and Philipson, K. D. (2001) Split Na^+-Ca^{2+} exchangers. Implications for function and expression, *J. Biol. Chem. 276*, 19603−19609.
10. Qiu, Z., Chen, J., Nicoll, D. A., and Philipson, K. D. (2001) A disulfide bond is required for functional assembly of NCX1 from complementary fragments, *Biochem. Biophys. Res. Commun. 287*, 825−828.
11. Li, X. F., and Lytton, J. (1999) A circularized sodium-calcium exchanger exon 2 transcript, *J. Biol. Chem. 274*, 8153−8160.
12. Van Eylen, F., Kamagate, A., and Herchuelz, A. (2001) A new Na/Ca exchanger splicing pattern identified in situ leads to a functionally active 70kDa NH(2)-terminal protein, *Cell Calcium 30*, 191−198.
13. Gabellini, N., Bortoluzzi, S., Danieli, G. A., and Carafoli, E. (2002) The human SLC8A3 gene and the tissue-specific Na^+/Ca^{2+} exchanger 3 isoforms, *Gene 298*, 1−7.
14. Green, W. N., and Millar, N. S. (1995) Ion-channel assembly, *Trends Neurosci. 18*, 280−287.
15. Fink, M., Duprat, F., Heurteaux, C., Lesage, F., Romey, G., Barhanin, J., and Lazdunski, M. (1996) Dominant negative chimeras provide evidence for homo and heteromultimeric assembly of inward rectifier K^+ channel proteins via their N-terminal end, *FEBS Lett. 378*, 64−68.
16. Salah, Z., Maoz, M., Cohen, I., Pizov, G., Pode, D., Runge, M. S., and Bar-Shavit, R. (2005) Identification of a novel functional androgen response element within hPar1 promoter: implications to prostate cancer progression, *FASEB J. 19*, 62−72.
17. Low, W., Kasir, J., and Rahamimoff, H. (1993) Cloning of the rat heart Na^+-Ca^{2+} exchanger and its functional expression in HeLa cells, *FEBS Lett. 316*, 63−67.
18. Jurman, M. E., Boland, L. M., Liu, Y., and Yellen, G. (1994) Visual identification of individual transfected cells for electrophysiology using antibody-coated beads, *BioTechniques 17*, 876−881.
19. Chernysh, O., Condrescu, M., and Reeves, J. P. (2004) Calcium-dependent regulation of calcium efflux by the cardiac sodium/calcium exchanger, *Am. J. Physiol. Cell Physiol. 287*, C797−C806 (Epub 2004 May 19).
20. Kang, K. J., Shibukawa, Y., Szerencsei, R. T., and Schnetkamp, P. P. (2005) Substitution of a single residue, Asp575, renders the NCKX2 K^+-dependent Na^+/Ca^{2+} exchanger independent of K^+, *J Biol. Chem. 280*, 6834−9 (Epub 2004 Dec 15).
21. Nitzan, Y. B., Sekler, I., Hershfinkel, M., Moran, A., and Silverman, W. F. (2002) Postnatal regulation of ZnT-1 expression in the mouse brain, *Brain Res. Dev. Brain Res. 137*, 149−157.
22. Kim, B. E., Wang, F., Dufner-Beattie, J., Andrews, G. K., Eide, D. J., and Petris, M. J. (2004) Zn^{2+}-stimulated endocytosis of the mZIP4 zinc transporter regulates its location at the plasma membrane, *J. Biol. Chem. 279*, 4523−4530.
23. Wang, F., Dufner-Beattie, J., Kim, B. E., Petris, M. J., Andrews, G., and Eide, D. J. (2004) Zinc-stimulated endocytosis controls activity of the mouse ZIP1 and ZIP3 zinc uptake transporters, *J. Biol. Chem. 279*, 24631−24639.
24. Reeves, J. P., and Condrescu, M. (2003) Allosteric activation of sodium-calcium exchange activity by calcium: persistence at low calcium concentrations, *J. Gen. Physiol. 122*, 621−639.
25. Kraev, A., Quednau, B. D., Leach, S., Li, X. F., Dong, H., Winkfein, R., Perizzolo, M., Cai, X., Yang, R., Philipson, K. D., and Lytton, J. (2001) Molecular cloning of a third member of the potassium-dependent sodium-calcium exchanger gene family, NCKX3, *J. Biol. Chem. 276*, 23161−23172.
26. Iwamoto, T., Kita, S., Uehara, A., Inoue, Y., Taniguchi, Y., Imanaga, I., and Shigekawa, M. (2001) Structural domains influencing sensitivity to isothiourea derivative inhibitor KB-R7943 in cardiac Nna(+)/Ca(2+) exchanger, *Mol. Pharmacol. 59*, 524−531.
27. Iwamoto, T., Kita, S., Uehara, A., Imanaga, I., Matsuda, T., Baba, A., and Katsuragi, T. (2004) Molecular determinants of Na^+/Ca^{2+} exchange (NCX1) inhibition by SEA0400, *J. Biol. Chem. 279*, 7544−7553 (Epub 2003 Dec 05).
28. Nicoll, D. A., Hryshko, L. V., Matsuoka, S., Frank, J. S., and Philipson, K. D. (1996) Mutation of amino acid residues in the putative transmembrane segments of the cardiac sarcolemmal Na^+-Ca^{2+} exchanger, *J. Biol. Chem. 271*, 13385−13391.
29. Arakawa, N., Katsuyama, M., Matsuno, K., Urao, N., Tabuchi, Y., Okigaki, M., Matsubara, H., and Yabe-Nishimura, C. (2006) Novel transcripts of NOX1 is regulated by alternative promoters and expressed under phenotypic modulation of vascular smooth muscle cells, *Biochem. J. 26*, 26.
30. Yerushalmi, H., Lebendiker, M., and Schuldiner, S. (1996) Negative dominance studies demonstrate the oligomeric structure of EmrE, a multidrug antiporter from *Escherichia coli*, *J. Biol. Chem. 271*, 31044−31048.
31. Wang, C., Hu, H. Z., Colton, C. K., Wood, J. D., and Zhu, M. X. (2004) An alternative splicing product of the murine trpv1 gene dominant negatively modulates the activity of TRPV1 channels, *J. Biol. Chem. 279*, 37423−37430.
32. MacKinnon, R. (1991) Determination of the subunit stoichiometry of a voltage-activated potassium channel, *Nature 350*, 232−235.
33. Philipson, K. D., and Nicoll, D. A. (2000) Sodium-calcium exchange: a molecular perspective, *Annu. Rev. Physiol. 62*, 111−133.

34. Cai, X., and Lytton, J. (2004) The cation/Ca(2+) exchanger superfamily: phylogenetic analysis and structural implications, *Mol. Biol. Evol. 21*, 1692−1703.
35. Iwamoto, T., Uehara, A., Imanaga, I., and Shigekawa, M. (2000) The Na^+/Ca^{2+} exchanger NCX1 has oppositely oriented reentrant loop domains that contain conserved aspartic acids whose mutation alters its apparent Ca^{2+} affinity, *J. Biol. Chem. 275*, 38571−38580.
36. Pornillos, O., Chen, Y. J., Chen, A. P., and Chang, G. (2005) X-ray structure of the EmrE multidrug transporter in complex with a substrate, *Science 310*, 1950−1953.
37. Bowie, J. U. (2006) Flip-flopping membrane proteins, *Nat. Struct. Mol. Biol. 13*, 94−96.
38. Rapp, M., Granseth, E., Seppala, S., and von Heijne, G. (2006) Identification and evolution of dual-topology membrane proteins, *Nat. Struct. Mol. Biol. 13*, 112−116.
39. Zhorov, B. S., and Tikhonov, D. B. (2004) Potassium, sodium, calcium and glutamate-gated channels: pore architecture and ligand action, *J. Neurochem. 88*, 782−799.
40. Claros, M. G., and von Heijne, G. (1994) TopPred II: an improved software for membrane protein structure predictions, *Comput. Appl. Biosci. 10*, 685−686.

BI060633B